

Position Domain Integrity Analysis for Generalized Integer Aperture Bootstrapping

G. Nathan Green, *The University of Texas at Austin*
Dr. Todd Humphreys, *The University of Texas at Austin*

Abstract—A full analysis of position domain integrity is carried out for the recently-introduced Generalized Integer Aperture Bootstrapping (GIAB) technique, a data-driven method for resolving and validating GNSS carrier-phase integer ambiguities suitable for high-integrity, safety-critical systems. The analysis can be extended to all integer aperture (IA) techniques that are generalized in the sense of allowing partial integer fixing. It is shown that generalized IA methods produce relative position (baseline) estimates that suffer from non-negligible biases. Key conditional distributions of the baseline computed from GIAB-validated ambiguities are rigorously derived for both full and partial ambiguity resolution. These distributions enable evaluation of the *a posteriori* risk from bias in the GIAB baseline estimate. Compared to EPIC, the state-of-the-art high-integrity algorithm, GIAB is shown to satisfy tighter integrity requirements for the same measurement model.

Keywords—Generalized integer aperture, bootstrap, CDGNSS, integrity, availability, partial ambiguity resolution, data-driven, EPIC, GERAFS

I. INTRODUCTION

The required navigation performance for carrier-phase differential global navigation satellite systems (CDGNSS) has become more demanding with each new application. Performance is assessed in terms of integrity, accuracy, and availability, among other metrics. Integrity is specified in terms of integrity risk IR , the probability that the solution error exceeds an alert limit AL without warning. Accuracy can be specified in terms of quantiles of interest, such as 95% accuracy, which refers to the error volume within which 95% of solutions fall. Availability is the percentage of time that the solution satisfies its required integrity and accuracy.

The ground-based augmentation system (GBAS), originally specified over a decade ago as a landing aid for large runways on land, calls for vertical AL s of 10 m with IR on the order of 10^{-7} per approach. Under zero-mean-error Gaussian assumptions, this leads to a relatively loose 95% accuracy requirement of 2 m, which can be met by a float CDGNSS solution, though the accuracy and integrity were specified independently. More recent navigation system applications, such as landing aboard an aircraft carrier and a recent demonstration of autonomous aerial refueling, have meter-level AL s, IR on the order of 10^{-6} , and decimeter-level accuracy requirements. Such a stringent performance specification can only be met by CDGNSS positioning when the carrier-phase ambiguities are resolved, i.e. fixed, as integers.

Emerging uses of CDGNSS include fully autonomous operation of large unmanned aerial vehicles (UAVs) from aircraft carriers, which will demand IR on the order of 10^{-7} with

AL s of about 1 m and decimeter-level accuracy. For these demanding new applications to achieve the required navigation performance, it will be essential to verifiably control the risk from incorrect ambiguity resolution by eliminating or bounding any induced biases in the three-dimensional relative position, or baseline, solution.

State-of-the-art methods in high-integrity CDGNSS enforce IR constraints in the position domain by accounting for baseline biases induced by incorrect integer fixing. Two such methods are the Geometry Extra Redundant Almost Fixed Solutions (GERAFS) [1] and the Enforced Position domain Integrity-risk of Cycle resolution (EPIC) [2]–[5] algorithms. Both of these rely exclusively on *a priori* error models to determine, before the measurements are processed, whether a fixed solution or a float backup solution will be selected. This approach is termed model-driven because the solution selection logic is entirely dependent on the prior error model. Given conservative error models, because GERAFS and EPIC attempt to bound IR using the *a priori* distribution, they are inherently conservative. Their conservatism arises from the need to protect against position domain biases induced by a large number of potentially-incorrect fixes without the benefit of conditioning on the observed carrier-phase measurements. The development and validation of such conservative error models is a separate and significant effort [6].

In contrast to the model-driven approach, data-driven methods exploit measured data to decide whether to accept the fixed or float solution. Conditioning selection on the observed measurements reduces the risk of incorrect ambiguity resolution. Foremost among data-driven techniques is the integer aperture (IA) approach [7]. In this approach, the integer ambiguity vector is first estimated by some means, e.g., integer bootstrapping (IB) [8] or integer least squares (ILS) [9], after which a test statistic is computed from the ambiguity residual, i.e., the difference between the float and fixed ambiguities. Based on this statistic, a hypothesis test decides whether to accept or reject the fixed solution.

IA bootstrapping (IAB) is a particularly simple type of IA estimation in which the integer ambiguities are fixed via IB and the test statistic is produced by a second application of IB, this time to a scaled-up version of the ambiguity residual [10]. If the statistic is the zero vector, the fixed solution is selected; otherwise the float solution is selected. IAB is sub-optimal in two respects: First, IB does not always find the maximum likelihood integer ambiguity, as opposed to ILS, which is guaranteed to do so. Second, IAB fails to maximize the probability of successfully fixing the ambiguities for a given

probability of incorrectly fixing them. Although sub-optimal, IB enjoys a significant advantage: its fixing probabilities are analytically calculable, which allows the residual scaling parameter to be set analytically as a function of a desired probability of incorrect fix, or failure rate, \bar{P}_F . Crucially, this property enables a system to provably satisfy the strict performance requirements of safety-of-life applications.

A companion paper [11] extends the IAB technique to a generalized form, called Generalized Integer Aperture Bootstrapping (GIAB), in which subsets of the full integer ambiguity set are considered for resolution if the full set cannot be fixed confidently. Salient features of GIAB are (1) the probability of incorrect ambiguity resolution, P_F , is analytically computable, (2) the probability of correctly resolving any of the considered subsets of ambiguities, P_{S_i} , is also analytically computable, and (3) the integer aperture test thresholds can be set analytically to bound P_F while nearly maximizing P_{S_m} , where m is the number of integer ambiguities to be estimated.

It was noted in [11] that the conditional distribution of the integer-constrained baseline estimate produced by GIAB exhibits non-negligible biases, even when all fixed integers pass validation. No prior work has characterized these biases or assessed their effect on integrity risk. Subsequent to the preliminary version of this paper [12], it was shown that combined estimation-with-exclusion methods exhibit biases when certain symmetry properties of the test statistic and exclusion regions are not maintained, even when conditioned on correct exclusion [13]. This general property was then demonstrated in receiver autonomous integrity monitoring with exclusion. This paper shows that, even though GIAB with partial fixing satisfies the symmetry conditions of [13] and produces a zero-mean-error baseline estimate, the distribution is multi-modal without a mode at zero-error. Whereas [13] addressed only the first moment of the distribution of the combined exclusion-estimation output, this paper addresses the full probability density under several conditions and Gaussian assumptions.

This paper, which extends a preliminary version presented in [12], makes four novel contributions to the literature: First, it shows that baseline estimate biases are present in any data-driven partial ambiguity resolution algorithm that corrects the float baseline with the validated fixes. Second, it develops and validates an analytical characterization of several important conditional distributions of the GIAB baseline. Third, it extends the position domain integrity concepts originally developed for EPIC to data-driven algorithms for use in safety-of-life applications. Fourth, it validates GIAB's performance via Monte Carlo simulation and compares this with EPIC.

II. GENERALIZED INTEGER APERTURE BOOTSTRAPPING

To make this paper self-contained, this section presents a digest of portions of the companion paper [11]. Proofs of the companion paper's results are given therein.

GIAB begins by computing the so-called float solution from the linearized, short-baseline GNSS measurement model

$$\mathbf{y} = B\mathbf{b} + A\mathbf{a} + \boldsymbol{\nu} \quad (1)$$

where $\mathbf{y} \in \mathbb{R}^n$ contains the ‘‘observed-minus-modeled’’ double-difference carrier-phase and, optionally, pseudorange

measurements, $\mathbf{b} \in \mathbb{R}^3$ is the unknown, real-valued correction to the modeled baseline between GNSS antennas, $\mathbf{a} \in \mathbb{Z}^m$ holds the unknown carrier phase integer ambiguities, B and A are appropriately-dimensioned measurement sensitivity matrices, and $\boldsymbol{\nu} \in \mathbb{R}^n$ is zero-mean, double-difference measurement noise with variance $Q_{\mathbf{y}}$.

Applying weighted least squares estimation to (1), with $H = [B \ A]$, produces real-valued estimates of \mathbf{b} and \mathbf{a} :

$$\begin{bmatrix} \hat{\mathbf{b}} \\ \hat{\mathbf{a}} \end{bmatrix} = (H^T Q_{\mathbf{y}}^{-1} H)^{-1} H^T Q_{\mathbf{y}}^{-1} \mathbf{y} \quad (2a)$$

$$E \left(\begin{bmatrix} \hat{\mathbf{b}} \\ \hat{\mathbf{a}} \end{bmatrix} \right) = \begin{bmatrix} \mathbf{b} \\ \mathbf{a} \end{bmatrix} \quad (2b)$$

$$\text{cov} \left(\begin{bmatrix} \hat{\mathbf{b}} \\ \hat{\mathbf{a}} \end{bmatrix} \right) = \begin{bmatrix} Q_{\hat{\mathbf{b}}} & Q_{\hat{\mathbf{b}}\hat{\mathbf{a}}} \\ Q_{\hat{\mathbf{a}}\hat{\mathbf{b}}} & Q_{\hat{\mathbf{a}}} \end{bmatrix} = (H^T Q_{\mathbf{y}}^{-1} H)^{-1} \quad (2c)$$

The estimates $\hat{\mathbf{a}} \in \mathbb{R}^m$ and $\hat{\mathbf{b}} \in \mathbb{R}^3$, called the float ambiguity and float baseline, ignore the integer constraint $\mathbf{a} \in \mathbb{Z}^m$.

Next, the float ambiguities are decorrelated using the commonly accepted LAMBDA method [14], [15]. The decorrelated float ambiguity is $\hat{\mathbf{z}} = Z^T \hat{\mathbf{a}}$, and the transformed true ambiguity is $\mathbf{z} = Z^T \mathbf{a}$, with Z being the integer-preserving transformation matrix. Likewise, $Q_{\hat{\mathbf{a}}}$ and $Q_{\hat{\mathbf{b}}\hat{\mathbf{a}}}$ are transformed as $Q_{\hat{\mathbf{z}}} = Z^T Q_{\hat{\mathbf{a}}} Z$ and $Q_{\hat{\mathbf{b}}\hat{\mathbf{z}}} = Q_{\hat{\mathbf{b}}\hat{\mathbf{a}}} Z$. All integer-related operations hereafter will be performed in the decorrelated space, with $\hat{\mathbf{z}}$ referred to as the float ambiguity.

GIAB's objective is to fix and validate as many of the ambiguities as possible while ensuring that the probability that a validated ambiguity is incorrect is less than a specified level, \bar{P}_F . GIAB outputs the number of validated ambiguities, $q \in \{0, \dots, m\}$, and the vector, $\hat{\mathbf{z}} \in \mathbb{Z}^{\min(q+1, m)}$, whose first q elements are the fixed and validated ambiguities, and whose $(q+1)$ th element, if $q < m$, is the first fixed but rejected ambiguity.

The outputs of GIAB can be mapped to various events defined in terms of the random variables $\hat{\mathbf{z}}$ and q . In the following event definitions, $\mathbf{z}_{1:n}$ indicates the vector composed of the first n elements of the vector \mathbf{z} :

$$F : \hat{\mathbf{z}}_{1:q} \neq \mathbf{z}_{1:q}, \quad q \in \{1, \dots, m\} \quad (3a)$$

$$U : q = 0 \quad (3b)$$

$$S_i : \hat{\mathbf{z}}_{1:i} = \mathbf{z}_{1:i}, \quad q = i \in \{1, \dots, m\} \quad (3c)$$

$$Z_i : \hat{\mathbf{z}}_{1:i} = \mathbf{z}_{1:i}, \quad q = i \in \{0, \dots, m\} \quad (3d)$$

$$CF_i : \hat{\mathbf{z}}_{1:i} = \mathbf{z}_{1:i}, \quad i \in \{1, \dots, m\} \quad (3e)$$

$$R_{i+1} : q = i < m \quad (3f)$$

The failure event F occurs upon validation of any incorrect integers. The undecided event U occurs when no ambiguity is fixed. There are m success events S_i defined for each possible number of correctly validated integer fixes from 1 to m . The event Z_i is identical to S_i except that it includes the $q = 0$ (no fixes) case. Note that the null vector $\hat{\mathbf{z}}_{1:0}$ is assumed to be identical to $\mathbf{z}_{1:0}$ so that $Z_0 = U$. The correct fix event CF_i occurs when the first $i \geq 1$ integers are fixed correctly, irrespective of the value of q . The rejection event R_{i+1} occurs when GIAB refuses to fix the $(i+1)$ th ambiguity.

GIAB requires that the variance of the float ambiguity be decomposed into LDL^T form such that

$$Q_{\hat{z}} = LDL^T \quad (4)$$

where L is a unit-lower triangular matrix and D is a diagonal matrix. The float ambiguity can be modeled as the true ambiguity plus zero-mean Gaussian noise, $\hat{z} = z + \epsilon$, $\epsilon \sim \mathcal{N}(0, Q_{\hat{z}})$. Multiplication by L^{-1} transforms ϵ into a vector whose elements are mutually uncorrelated: $\epsilon_c \triangleq L^{-1}\epsilon$, $\epsilon_c \sim \mathcal{N}(0, D)$. The quantity ϵ_c , called the decorrelated float ambiguity error, plays a key role in the analysis that follows. Again, this assumption depends on the existence of a validated model for the measurements. If measurements are taken over multiple epochs, their correlations must be perfectly known for complete decorrelation. This paper studies single epoch ambiguity resolution to eliminate time correlation effects.

GIAB takes as input a vector, β , called the aperture parameter vector, that determines the validation threshold for each ambiguity. β also determines the probabilities of the failure, success, and undecided events, P_F , P_{S_i} , and P_U . β is set as a function of D that ensures $P_F < \bar{P}_F$. GIAB can be represented as the function

$$[q, \hat{z}] = \text{GIAB}(\hat{z}, L, \beta) \quad (5)$$

The event probabilities are [11]

$$P_F = P_{E1} + \sum_{i=2}^m P_{Ei} \prod_{j=1}^{i-1} P_{Cj} \quad (6a)$$

$$P_{S_i} = \begin{cases} \prod_{j=1}^m P_{Cj} & i = m \\ P_{R(i+1)} \prod_{j=1}^i P_{Cj} & i \in \{1, \dots, m-1\} \end{cases} \quad (6b)$$

$$P_U = P_{R1} \quad (6c)$$

where, with $\Phi(x)$ being the standard normal cumulative distribution function,

$$P_{Ci} = 2\Phi\left(\frac{\beta_i/2}{\sqrt{d_i}}\right) - 1 \quad (7a)$$

$$P_{Ei} = \sum_{\zeta \in \mathbb{Z} \setminus \{0\}} \left(\Phi\left(\frac{\beta_i/2 - \zeta}{\sqrt{d_i}}\right) - \Phi\left(\frac{-\beta_i/2 - \zeta}{\sqrt{d_i}}\right) \right) \quad (7b)$$

$$P_{Ri} = 1 - P_{Ei} - P_{Ci} \quad (7c)$$

An upper bound on P_{Ei} that leads to an interesting upper bound on P_F is obtained by assuming all float ambiguity errors larger than $1 - \frac{\beta_i}{2}$ cause an error, even though some will actually be rejected:

$$P_{Ei} \leq 2\Phi\left(\frac{\beta_i/2 - 1}{\sqrt{d_i}}\right) \quad (8)$$

This bound is used to compute the aperture parameter β .

Let $r = \min\{q+1, m\}$ for notational simplicity. The ambiguity residual is defined as $\tilde{\epsilon} \triangleq \hat{z}_{1:r} - \hat{z}$. Note that if $\hat{z} = z_{1:r}$, then $\tilde{\epsilon} = \epsilon$. Denote the upper $r \times r$ sub-matrix of L as $L_{1:r,1:r}$. An important quantity, called the sequentially-constrained ambiguity residual, is defined as $\tilde{\epsilon}_c \triangleq L_{1:r,1:r}^{-1}\tilde{\epsilon}$.

This vector has a convenient property derived from the chosen LDL^T decomposition: if the first i integer ambiguities GIAB fixes are correctly fixed (i.e., if $\hat{z}_{1:i} = z_{1:i}$), then the $(i+1)$ th element of $\tilde{\epsilon}_c$, denoted $\tilde{\epsilon}_{c(i+1)}$, is uncorrelated with the previous i elements. This property will be exploited later on. GIAB decides whether to fix the i th ambiguity based on the value of $\tilde{\epsilon}_{ci}$. It operates in such a way that

$$\begin{aligned} |\tilde{\epsilon}_{ci}| &\leq \frac{\beta_i}{2} && \text{for } i \in \{1, \dots, q\}, q > 0 \\ \frac{\beta_i}{2} < |\tilde{\epsilon}_{ci}| &\leq \frac{1}{2} && \text{for } i = q+1, q < m \end{aligned} \quad (9)$$

In other words, all $i \in \{1, \dots, q\}$ ambiguities that GIAB validates have small sequentially-constrained ambiguity residuals $\tilde{\epsilon}_{ci}$, but the $(q+1)$ th ambiguity, which GIAB refuses to fix (assuming $q < m$), has $\tilde{\epsilon}_{c(q+1)}$ too large for GIAB to confidently fix. Note that a rounding operation within GIAB ensures $|\tilde{\epsilon}_{ci}| \leq 1/2$.

If the full set of ambiguities is fixed and validated, the float baseline can be constrained by the float ambiguity residual, resulting in the so-called fixed baseline estimate:

$$\begin{aligned} \hat{\mathbf{b}} &= \hat{\mathbf{b}} - Q_{\hat{\mathbf{b}}\hat{\mathbf{z}}} Q_{\hat{\mathbf{z}}}^{-1} \tilde{\epsilon} \\ &= \hat{\mathbf{b}} - Q_{\hat{\mathbf{b}}\hat{\mathbf{z}}} (L^{-T} D^{-1} L^{-1}) L \tilde{\epsilon}_c \\ &= \hat{\mathbf{b}} - Q_{\hat{\mathbf{b}}\hat{\mathbf{z}}} L^{-T} D^{-1} \tilde{\epsilon}_c \\ &= \hat{\mathbf{b}} - Q_{\hat{\mathbf{b}}\hat{\mathbf{z}}_c} D^{-1} \tilde{\epsilon}_c \end{aligned} \quad (10)$$

where $Q_{\hat{\mathbf{b}}\hat{\mathbf{z}}_c} \triangleq Q_{\hat{\mathbf{b}}\hat{\mathbf{z}}} L^{-T}$.

The distribution of the fully-fixed baseline conditioned on a particular fixed ambiguity $\hat{z} = z + \Delta z$ is [16]

$$(\hat{\mathbf{b}} | \hat{z} = z + \Delta z) \sim \mathcal{N}(\mathbf{b} + Q_{\hat{\mathbf{b}}\hat{\mathbf{z}}} Q_{\hat{\mathbf{z}}}^{-1} \Delta z, Q_{\hat{\mathbf{b}}}) \quad (11)$$

where $Q_{\hat{\mathbf{b}}} \triangleq Q_{\hat{\mathbf{b}}} - Q_{\hat{\mathbf{b}}\hat{\mathbf{z}}_c} D^{-1} Q_{\hat{\mathbf{b}}\hat{\mathbf{z}}_c}^T$. Thus, when the integer ambiguity is fixed correctly ($\Delta z = \mathbf{0}$), the fully-fixed baseline has a Gaussian distribution whose mean equals the true baseline \mathbf{b} .

III. PRIOR DISTRIBUTION OF THE GENERALIZED INTEGER APERTURE BASELINE

Analogous to the float baseline $\hat{\mathbf{b}}$ and the fixed baseline $\check{\mathbf{b}}$, a partially-fixed baseline, denoted $\tilde{\mathbf{b}}$, can be calculated from the inputs and outputs of GIAB. The *a priori* and *a posteriori* distributions of $\tilde{\mathbf{b}}$ are important performance indicators. This section derives the *a priori* distribution of $\tilde{\mathbf{b}}$.

Let $Q_{\hat{\mathbf{b}}\hat{\mathbf{z}}_{cj}}$ indicate the j th column of the matrix $Q_{\hat{\mathbf{b}}\hat{\mathbf{z}}_c}$, and d_j the j th entry on the diagonal of D . Because D is diagonal, (10) can be written

$$\tilde{\mathbf{b}} = \hat{\mathbf{b}} - \sum_{j=1}^m Q_{\hat{\mathbf{b}}\hat{\mathbf{z}}_{cj}} \frac{\tilde{\epsilon}_{cj}}{d_j} \quad (12)$$

The baseline constrained by only the first i ambiguities, written $\tilde{\mathbf{b}}_i$, can be calculated by truncating the summation in (12) at i :

$$\tilde{\mathbf{b}}_i = \hat{\mathbf{b}} - \sum_{j=1}^i Q_{\hat{\mathbf{b}}\hat{\mathbf{z}}_{cj}} \frac{\tilde{\epsilon}_{cj}}{d_j} \quad (13)$$

The event $q = i < m$ implies that GIAB could not fix the $(i+1)$ th ambiguity without violating the specified probability

of failure. For the moment, let $\bar{\mathbf{b}} = \check{\mathbf{b}}_q$ be GIAB's partially-fixed baseline solution; alternative assignments for $\bar{\mathbf{b}}$ will be explored later on. Denote by F^c the complement of the failure event, F , and let $f_{\bar{\mathbf{b}}|F}$ and $f_{\bar{\mathbf{b}}|F^c}$ be the probability density functions (PDFs) of $\bar{\mathbf{b}}$ conditioned respectively on F and F^c . It follows from the total probability theorem that the prior (unconditioned) PDF of the partially-fixed baseline $\bar{\mathbf{b}}$ is

$$f_{\bar{\mathbf{b}}}(\boldsymbol{\xi}) = f_{\bar{\mathbf{b}}|F^c}(\boldsymbol{\xi})(1 - P_F) + f_{\bar{\mathbf{b}}|F}(\boldsymbol{\xi})P_F \quad (14)$$

Since, by design, $P_F \leq \bar{P}_F \ll 1$, momentarily neglect the second term on the right-hand side of (14). This term is not important for the average performance of the GIAB algorithm, though it is central to position domain integrity considerations in Section VII. A detailed expression for $f_{\bar{\mathbf{b}}|F^c}(\boldsymbol{\xi})$, from the first term, is derived along with other conditional PDFs in the following section.

IV. CONDITIONAL DISTRIBUTIONS OF THE GENERALIZED INTEGER APERTURE BASELINE

Various conditional distributions of $\bar{\mathbf{b}}$ offer valuable insight into its behavior under partial ambiguity resolution. This section presents a conceptual overview of the various distributions, followed by detailed derivations of the same.

A. Conceptual Overview

Consider $f_{\bar{\mathbf{b}}|CF_i}(\boldsymbol{\xi})$, the PDF of $\bar{\mathbf{b}}$ conditioned on GIAB correctly resolving the first i ambiguities. Note that this conditioning makes no assumption that GIAB resolved *only* i ambiguities; in fact, GIAB may have resolved more than i —correctly or not. The conditioning on CF_i assumes only that the first i were correctly resolved. One would expect this conditional PDF to be Gaussian with a mean of \mathbf{b} , since, as (11) indicates, the fully-fixed baseline $\bar{\mathbf{b}}$ conditioned on $\Delta z = 0$ is Gaussian with mean \mathbf{b} . Indeed, this turns out to be the case.

Now consider $f_{\bar{\mathbf{b}}|Z_i}(\boldsymbol{\xi})$ for $i < m$. The event Z_i implies $\check{\mathbf{z}}_{1:i} = \mathbf{z}_{1:i}$ but when $i < m$ it further implies that GIAB refused to fix one or more ambiguities. Thus, conditioning on Z_i when $i < m$ indicates that the magnitude of the $(i+1)$ th sequentially-constrained ambiguity residual $\check{\epsilon}_{c(i+1)}$ was larger than $\beta_{i+1}/2$. No assumption is made about the particular value of $\check{\epsilon}_{c(i+1)}$, only that it was too large to confidently fix the corresponding integer. In this case will $f_{\bar{\mathbf{b}}|Z_i}(\boldsymbol{\xi})$ be Gaussian with mean \mathbf{b} ? The answer is no: $f_{\bar{\mathbf{b}}|Z_i}(\boldsymbol{\xi})$ has mean \mathbf{b} but is not Gaussian. This can be explained by considering (13) and recognizing that, although $\check{\epsilon}_{c(i+1)}$ being large has no bearing on $\check{\epsilon}_{c_j}$ for $j \in \{1, \dots, i\}$ (because these are uncorrelated with $\check{\epsilon}_{c(i+1)}$ under Z_i), it *does* imply something about $\bar{\mathbf{b}}$, namely, that its PDF does not have a mode at \mathbf{b} : the most probable values of $\bar{\mathbf{b}}$ are offset from \mathbf{b} .

Finally, consider $f_{\bar{\mathbf{b}}|\check{\epsilon}_{c(i+1)}, Z_i}(\boldsymbol{\xi}|\varepsilon)$, which is the PDF of $\bar{\mathbf{b}}$ conditioned on Z_i for $i < m$ and on the particular value of the sequentially-constrained ambiguity residual, $\check{\epsilon}_{c(i+1)}$, that caused GIAB to refuse to fix the $(i+1)$ th ambiguity. Somewhat surprisingly, this PDF turns out to be neither Gaussian nor of mean \mathbf{b} . This key result, unknown in the existing literature, is critical because $f_{\bar{\mathbf{b}}|\check{\epsilon}_{c(i+1)}, Z_i}(\boldsymbol{\xi}|\varepsilon)$ informs decision making

about $\bar{\mathbf{b}}$: it is the best indicator of whether a particular $\bar{\mathbf{b}}$ will be accurate enough for a high-integrity application.

Manipulation in the following subsections leads to detailed expressions for $f_{\bar{\mathbf{b}}|F^c}(\boldsymbol{\xi})$, $f_{\bar{\mathbf{b}}|Z_i}(\boldsymbol{\xi})$, and $f_{\bar{\mathbf{b}}|\check{\epsilon}_{c(i+1)}, Z_i}(\boldsymbol{\xi}|\varepsilon)$.

B. Finding $f_{\bar{\mathbf{b}}|F^c}$

The conditional PDF $f_{\bar{\mathbf{b}}|F^c}$, which appears in (14), can be written in terms of $f_{\bar{\mathbf{b}}|Z_i}(\boldsymbol{\xi})$, the PDF of $\bar{\mathbf{b}}$ conditioned on successful validation of $q = i$ ambiguities, as follows:

$$\begin{aligned} f_{\bar{\mathbf{b}}|F^c}(\boldsymbol{\xi}) &= \sum_{i=0}^m P(Z_i|F^c) f_{\bar{\mathbf{b}}|Z_i}(\boldsymbol{\xi}) \\ &= \sum_{i=0}^m \frac{P(Z_i, F^c)}{P(F^c)} f_{\bar{\mathbf{b}}|Z_i}(\boldsymbol{\xi}) \\ &= \sum_{i=0}^m \frac{P_{Z_i}}{1 - P_F} f_{\bar{\mathbf{b}}|Z_i}(\boldsymbol{\xi}) \end{aligned} \quad (15)$$

where P_{Z_i} is the probability of the event Z_i , and where the final simplification follows from $Z_i \subset F^c$.

C. Finding $f_{\bar{\mathbf{b}}|Z_i}(\boldsymbol{\xi})$

The PDF $f_{\bar{\mathbf{b}}|Z_i}(\boldsymbol{\xi})$, which appears in (15), can be expressed in terms of GIAB's output $\check{\mathbf{z}} \in \mathbb{Z}^r$, where $r = \min(m, q+1)$. When conditioned on Z_i with $i < m$, the first i ambiguities in $\check{\mathbf{z}}$, are correct, but the $(i+1)$ th may not be; in other words, $\check{\mathbf{z}} = [z_1, \dots, z_i, z_{i+1} + \Delta z]^T$ for some $\Delta z \in \mathbb{Z}$. Recalling that $\check{\epsilon}_c \triangleq L_{1:r, 1:r}^{-1}(\hat{\mathbf{z}}_{1:r} - \check{\mathbf{z}})$, and recognizing $L_{1:r, 1:r}^{-1}$ as unit lower triangular, then given Z_i it follows that $\check{\epsilon}_{c(1:i)} = \epsilon_{c(1:i)} \triangleq L_{1:i, 1:i}^{-1}(\hat{\mathbf{z}}_{1:i} - \mathbf{z}_{1:i})$ and that $\check{\epsilon}_{c(i+1)} = \epsilon_{c(i+1)} - \Delta z$. From standard probability theory, the PDF of the difference $\check{\epsilon}_{c(i+1)} = \epsilon_{c(i+1)} - \Delta z$ can be expressed in terms of the joint PDF of $\epsilon_{c(i+1)}$ and Δz , which, in turn can be expressed as the product of the conditional and marginal PDFs of Δz and $\epsilon_{c(i+1)}$, respectively:

$$\begin{aligned} f_{\check{\epsilon}_{c(i+1)}|Z_i}(\varepsilon) &= \sum_{k \in \mathbb{Z}} f_{\epsilon_{c(i+1)}, \Delta z|Z_i}(\varepsilon + k, k) \\ &= \sum_{k \in \mathbb{Z}} f_{\Delta z|\epsilon_{c(i+1)}, Z_i}(k|\varepsilon + k) f_{\epsilon_{c(i+1)}|Z_i}(\varepsilon + k) \end{aligned} \quad (16)$$

This expression can be simplified by noting from (9) that under Z_i the rejected sequentially-constrained ambiguity residual $\check{\epsilon}_{c(i+1)}$ satisfies

$$\frac{\beta_{i+1}}{2} < |\check{\epsilon}_{c(i+1)}| \leq \frac{1}{2}$$

Expressed another way, the support of $\check{\epsilon}_{c(i+1)}$ under Z_i is

$$A_{i+1} \triangleq \left\{ \varepsilon \left| \frac{\beta_{i+1}}{2} < |\varepsilon| \leq \frac{1}{2} \right. \right\}$$

Thus, given that $\check{\epsilon}_{c(i+1)} = \epsilon_{c(i+1)} - \Delta z \in A_{i+1}$, the conditioning on $\epsilon_{c(i+1)} = \varepsilon + k$ in (16) implies $\Delta z = k$. (The condition $|\varepsilon| = 1/2$ upsets this unique mapping but happens with probability 0.) Therefore,

$$f_{\Delta z|\epsilon_{c(i+1)}, Z_i}(k|\varepsilon + k) = 1 \quad \forall k \in \mathbb{Z}, \forall \varepsilon \in A_{i+1}$$

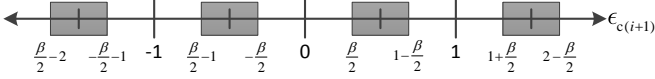


Fig. 1: The rejection event R_{i+1} is triggered when $\epsilon_{c(i+1)}$ falls within the indicated bands. For compactness, β_{i+1} is abbreviated as β .

and (16) simplifies to

$$f_{\check{\epsilon}_{c(i+1)}|Z_i}(\varepsilon) = \sum_{k \in \mathbb{Z}} f_{\epsilon_{c(i+1)}|Z_i}(\varepsilon + k) \quad (17)$$

With these preliminaries, $f_{\bar{\mathbf{b}}|Z_i}(\boldsymbol{\xi})$ can be constructed as the marginal of the joint PDF of $\bar{\mathbf{b}}$ and $\check{\epsilon}_{c(i+1)}$, and the latter can be expressed in terms of a sum of joint PDFs with $\epsilon_{c(i+1)}$ by the same reasoning that led to (17):

$$\begin{aligned} f_{\bar{\mathbf{b}}|Z_i}(\boldsymbol{\xi}) &= \int_{A_{i+1}} f_{\bar{\mathbf{b}}, \epsilon_{c(i+1)}|Z_i}(\boldsymbol{\xi}, \varepsilon) d\varepsilon \\ &= \int_{A_{i+1}} \sum_{k \in \mathbb{Z}} f_{\bar{\mathbf{b}}, \epsilon_{c(i+1)}|Z_i}(\boldsymbol{\xi}, \varepsilon + k) d\varepsilon \end{aligned} \quad (18)$$

D. Finding $f_{\bar{\mathbf{b}}, \epsilon_{c(i+1)}|Z_i}(\boldsymbol{\xi}, \varepsilon + k)$

To find $f_{\bar{\mathbf{b}}, \epsilon_{c(i+1)}|Z_i}(\boldsymbol{\xi}, \varepsilon + k)$, which appears in (18), it is helpful to express the rejection event R_{i+1} in terms of $\epsilon_{c(i+1)}$, as follows:

$$R_{i+1} : \epsilon_{c(i+1)} \in \{\varepsilon + k \mid \varepsilon \in A_{i+1}, k \in \mathbb{Z}\}$$

Fig. 1 illustrates the bands of $\epsilon_{c(i+1)}$ that trigger rejection. In the context of (18), where conditioning is on Z_i with $i < m$ [the $(i+1)$ th ambiguity was rejected], Z_i is the intersection of the correct fix event CF_i and the rejection event R_{i+1} . Accordingly, the PDF $f_{\bar{\mathbf{b}}, \epsilon_{c(i+1)}|Z_i}(\boldsymbol{\xi}, \varepsilon)$ is identical to $f_{\bar{\mathbf{b}}, \epsilon_{c(i+1)}|CF_i}(\boldsymbol{\xi}, \varepsilon)$ but with two modifications: (1) support of $\epsilon_{c(i+1)}$ is restricted to R_{i+1} , and (2) a normalization by $P_{R_{i+1}}$, given in (7c), is applied to ensure the PDF integrates to unity. Let $\mathbf{1}_{R_{i+1}}(\varepsilon)$ be the indicator function for the rejection event, equal to unity for those values of ε that trigger R_{i+1} , and zero otherwise. Then the joint PDF is

$$f_{\bar{\mathbf{b}}, \epsilon_{c(i+1)}|Z_i}(\boldsymbol{\xi}, \varepsilon) = \frac{\mathbf{1}_{R_{i+1}}(\varepsilon)}{P_{R_{i+1}}} f_{\bar{\mathbf{b}}, \epsilon_{c(i+1)}|CF_i}(\boldsymbol{\xi}, \varepsilon) \quad (19)$$

To find $f_{\bar{\mathbf{b}}, \epsilon_{c(i+1)}|CF_i}(\boldsymbol{\xi}, \varepsilon)$ note that, under the event CF_i , $\check{\mathbf{b}}_i$ and $\epsilon_{c(i+1)}$ are jointly Gaussian:

$$\begin{bmatrix} \check{\mathbf{b}}_i \\ \epsilon_{c(i+1)} \end{bmatrix} \Big| CF_i \sim \mathcal{N} \left(\begin{bmatrix} \boldsymbol{\xi} \\ \varepsilon \end{bmatrix}; \begin{bmatrix} \mathbf{b} \\ 0 \end{bmatrix}, Q_{\check{\mathbf{b}}_i \epsilon_{c(i+1)}} \right) \quad (20)$$

with

$$Q_{\check{\mathbf{b}}_i \epsilon_{c(i+1)}} = \begin{bmatrix} Q_{\check{\mathbf{b}}_i} & Q_{\check{\mathbf{b}}_i \check{\epsilon}_{c(i+1)}} \\ Q_{\check{\mathbf{b}}_i \check{\epsilon}_{c(i+1)}}^T & d_{i+1} \end{bmatrix} \quad (21)$$

where $Q_{\check{\mathbf{b}}_i \check{\epsilon}_{c(i+1)}}$ is the $(i+1)$ th column of $Q_{\check{\mathbf{b}}_i \check{\mathbf{z}}_c}$, introduced in (10), and

$$Q_{\check{\mathbf{b}}_i} = Q_{\check{\mathbf{b}}} - \sum_{j=1}^i \frac{1}{d_j} Q_{\check{\mathbf{b}} \check{\mathbf{z}}_c j} \left(Q_{\check{\mathbf{b}} \check{\mathbf{z}}_c j} \right)^T \quad (22)$$

is found by exploiting the independence of each element of ϵ_c . Then the conditional mean error of $\bar{\mathbf{b}} = \check{\mathbf{b}}_i$, given CF_i and $\epsilon_{c(i+1)} = \varepsilon + k$, follows from the standard expression for the Gaussian conditional mean:

$$\begin{aligned} \boldsymbol{\mu}_k(\varepsilon) &\triangleq E[\bar{\mathbf{b}} - \mathbf{b} \mid \epsilon_{c(i+1)} = \varepsilon + k, CF_i] \\ &= Q_{\check{\mathbf{b}} \check{\mathbf{z}}_c(i+1)} \left(\frac{\varepsilon + k}{d_{i+1}} \right) \end{aligned} \quad (23)$$

Its covariance is found by extending the summation in (22) to $(i+1)$:

$$\text{cov}(\bar{\mathbf{b}} \mid \epsilon_{c(i+1)} = \varepsilon + k, CF_i) = Q_{\check{\mathbf{b}}_{i+1}} \quad (24)$$

Hence the partially-fixed baseline $\bar{\mathbf{b}}$, when conditioned on $\epsilon_{c(i+1)}$ and CF_i , is Gaussian distributed and biased away from the true baseline \mathbf{b} by $\boldsymbol{\mu}_k(\varepsilon)$:

$$f_{\bar{\mathbf{b}}|\epsilon_{c(i+1)}, CF_i}(\boldsymbol{\xi}|\varepsilon + k) = \mathcal{N}(\boldsymbol{\xi}; \mathbf{b} + \boldsymbol{\mu}_k(\varepsilon), Q_{\check{\mathbf{b}}_{i+1}}) \quad (25)$$

Then, recognizing that $\epsilon_c \sim \mathcal{N}(0, D)$ implies

$$f_{\epsilon_{c(i+1)}|CF_i}(\varepsilon) = \mathcal{N}(\varepsilon; 0, d_{i+1}) \quad (26)$$

and factoring the joint PDF in (19) into its conditional-times-marginal form yields this subsection's desired PDF:

$$\begin{aligned} f_{\bar{\mathbf{b}}, \epsilon_{c(i+1)}|Z_i}(\boldsymbol{\xi}, \varepsilon + k) &= \\ \frac{\mathbf{1}_{R_{i+1}}(\varepsilon)}{P_{R_{i+1}}} \mathcal{N}(\boldsymbol{\xi}; \mathbf{b} + \boldsymbol{\mu}_k(\varepsilon), Q_{\check{\mathbf{b}}_{i+1}}) \mathcal{N}(\varepsilon + k; 0, d_{i+1}) \end{aligned} \quad (27)$$

Moreover, substituting (27) into (18), yields $f_{\bar{\mathbf{b}}|Z_i}$, and substituting (18) into (15) yields a detailed expression for $f_{\bar{\mathbf{b}}|F^c}$:

$$\begin{aligned} f_{\bar{\mathbf{b}}|F^c}(\boldsymbol{\xi}) &= \frac{P_{S_m}}{1 - P_F} \mathcal{N}(\boldsymbol{\xi}; \mathbf{b}, Q_{\check{\mathbf{b}}_m}) \\ &+ \sum_{i=0}^{m-1} \frac{P_{Z_i}/P_{R_{i+1}}}{1 - P_F} \\ &\times \sum_{k \in \mathbb{Z}} \int_{A_{i+1}} \mathcal{N}(\boldsymbol{\xi}; \mathbf{b} + \boldsymbol{\mu}_k(\varepsilon), Q_{\check{\mathbf{b}}_{i+1}}) \mathcal{N}(\varepsilon + k; 0, d_{i+1}) d\varepsilon \end{aligned}$$

E. Finding $f_{\bar{\mathbf{b}}|\check{\epsilon}_{c(i+1)}, Z_i}(\boldsymbol{\xi}|\varepsilon)$

After the foregoing steps, one can find the important PDF $f_{\bar{\mathbf{b}}|\check{\epsilon}_{c(i+1)}, Z_i}(\boldsymbol{\xi}|\varepsilon)$ starting with

$$f_{\bar{\mathbf{b}}|\check{\epsilon}_{c(i+1)}, Z_i}(\boldsymbol{\xi}|\varepsilon) = \frac{f_{\bar{\mathbf{b}}, \check{\epsilon}_{c(i+1)}|Z_i}(\boldsymbol{\xi}, \varepsilon)}{f_{\check{\epsilon}_{c(i+1)}|Z_i}(\varepsilon)} \quad (28)$$

Substituting the integrand of (18) for the numerator and (17) for the denominator yields

$$f_{\bar{\mathbf{b}}|\check{\epsilon}_{c(i+1)}, Z_i}(\boldsymbol{\xi}|\varepsilon) = \frac{\sum_{k \in \mathbb{Z}} f_{\bar{\mathbf{b}}, \epsilon_{c(i+1)}|Z_i}(\boldsymbol{\xi}, \varepsilon + k)}{\sum_{j \in \mathbb{Z}} f_{\epsilon_{c(i+1)}|Z_i}(\varepsilon + j)} \quad (29)$$

Now substituting (27) and (26), where the normalization for the rejection event cancels out, and constraining $\varepsilon \in A_{i+1}$ to eliminate the indicator functions, yields

$$\begin{aligned} f_{\bar{\mathbf{b}}|\check{\epsilon}_{c(i+1)}, Z_i}(\boldsymbol{\xi}|\varepsilon) &= \\ = \frac{\sum_{k \in \mathbb{Z}} \mathcal{N}(\boldsymbol{\xi}; \mathbf{b} + \boldsymbol{\mu}_k(\varepsilon), Q_{\check{\mathbf{b}}_{i+1}}) \mathcal{N}(\varepsilon + k; 0, d_{i+1})}{\sum_{j \in \mathbb{Z}} \mathcal{N}(\varepsilon + j; 0, d_{i+1})} \end{aligned} \quad (30)$$

This PDF can be interpreted as a mixture of Gaussian densities with different means but equal variances. The mixture probabilities are in fact the conditional probabilities that $\Delta z = k$ given the sequentially-constrained ambiguity residual $\check{\epsilon}_{c(i+1)}$ and the event Z_i :

$$\begin{aligned} p_k(\varepsilon) &\triangleq P(\Delta z = k | \check{\epsilon}_{c(i+1)} = \varepsilon \in A_{i+1}, Z_i) \\ &= \frac{\mathcal{N}(\varepsilon + k; 0, d_{i+1})}{\sum_{j \in \mathbb{Z}} \mathcal{N}(\varepsilon + j; 0, d_{i+1})}, \varepsilon \in A_{i+1} \end{aligned} \quad (31)$$

Simplifying (30) with the mixture probability notation of (31) yields, for $\varepsilon \in A_{i+1}$,

$$f_{\bar{\mathbf{b}}|\check{\epsilon}_{c(i+1)}, Z_i}(\boldsymbol{\xi}|\varepsilon) = \sum_{k \in \mathbb{Z}} p_k(\varepsilon) \cdot \mathcal{N}(\boldsymbol{\xi}; \mathbf{b} + \boldsymbol{\mu}_k(\varepsilon), Q_{\check{\mathbf{b}}_{i+1}}) \quad (32)$$

F. Discussion

Two important observations can be drawn from the foregoing conditional distributions. First consider (32). Note that $p_k(\varepsilon)$ and $\boldsymbol{\mu}_k(\varepsilon)$ are evaluated only for $\varepsilon \neq 0$, since $\varepsilon \in A_{i+1}$, which does not contain the origin. From (23), one observes that, for $\varepsilon \neq 0$ and assuming $Q_{\check{\mathbf{b}}_{i+1}}$ is nonzero, the bias $\boldsymbol{\mu}_k(\varepsilon)$ is nonzero for any value of $k \in \mathbb{Z}$. Thus, the means of the Gaussian PDFs that get summed in (32) are all shifted away from the true baseline \mathbf{b} . It is possible for a weighting function $p_k(\varepsilon)$ to be chosen to counteract this shifting and thereby restore symmetry in $f_{\bar{\mathbf{b}}|\check{\epsilon}_{c(i+1)}, Z_i}(\boldsymbol{\xi}|\varepsilon)$, but the actual weighting that applies, given by (31), does not do this. As a result, $f_{\bar{\mathbf{b}}|\check{\epsilon}_{c(i+1)}, Z_i}(\boldsymbol{\xi}|\varepsilon)$ is asymmetric about \mathbf{b} with respect to $\boldsymbol{\xi}$.

To be explicitly clear, the PDF of the partially-fixed baseline $\bar{\mathbf{b}} = \check{\mathbf{b}}_q$ that results from correction of the float baseline $\hat{\mathbf{b}}$ with GIAB-produced $\check{\epsilon}_{c_j}$, as in (13) with $i = q < m$, when conditioned on $\check{\epsilon}_{c(i+1)} = \varepsilon \in A_{i+1}$, will not have a mean coincident with the true baseline \mathbf{b} even when all validated ambiguity fixes are correct.

The second important observation is that, for $i < m$, $f_{\bar{\mathbf{b}}|Z_i}(\boldsymbol{\xi})$ given by (18) is symmetric about \mathbf{b} but lacks a mode at \mathbf{b} . To see this, note that $f_{\bar{\mathbf{b}}|Z_i}(\boldsymbol{\xi})$ can be written

$$f_{\bar{\mathbf{b}}|Z_i}(\boldsymbol{\xi}) = \int_{A_{i+1}} f_{\bar{\mathbf{b}}|\check{\epsilon}_{c(i+1)}, Z_i}(\boldsymbol{\xi}|\varepsilon) f_{\check{\epsilon}_{c(i+1)}|Z_i}(\varepsilon) d\varepsilon \quad (33)$$

with $f_{\bar{\mathbf{b}}|\check{\epsilon}_{c(i+1)}, Z_i}(\boldsymbol{\xi}|\varepsilon)$ given by (32) and $f_{\check{\epsilon}_{c(i+1)}|Z_i}(\varepsilon)$ by (17). The first of these, $f_{\bar{\mathbf{b}}|\check{\epsilon}_{c(i+1)}, Z_i}(\boldsymbol{\xi}|\varepsilon)$, is symmetric about \mathbf{b} when integrated over ε because both $p_k(\varepsilon)$ from (31) and $\boldsymbol{\mu}_k(\varepsilon)$ from (23) are symmetric about the origin with respect to ε when summed over all $k \in \mathbb{Z}$. The second, $f_{\check{\epsilon}_{c(i+1)}|Z_i}(\varepsilon)$, is symmetric about the origin with respect to ε because the summand $f_{\check{\epsilon}_{c(i+1)}|Z_i}(\varepsilon + k)$ of (17), with ε restricted to A_{i+1} , is simply a normalized version of $f_{\check{\epsilon}_{c(i+1)}|CF_i}(\varepsilon + k)$ from (26). Thus, since $f_{\check{\epsilon}_{c(i+1)}|CF_i}(\varepsilon + k)$ and A_{i+1} are symmetric with respect to ε , so is $f_{\check{\epsilon}_{c(i+1)}|Z_i}(\varepsilon)$. Taken together, these facts imply that $f_{\bar{\mathbf{b}}|Z_i}(\boldsymbol{\xi})$ is symmetric about \mathbf{b} . Critically however, the support A_{i+1} does not contain the origin, so $\boldsymbol{\mu}_k(\varepsilon) \neq 0$ for all $\varepsilon \in A_{i+1}$ and all $k \in \mathbb{Z}$. This implies that, although $f_{\bar{\mathbf{b}}|Z_i}(\boldsymbol{\xi})$ with $i < m$ is symmetric about \mathbf{b} , it does not have a mode at \mathbf{b} .

The above two observations can be understood intuitively as follows: GIAB's refusal to fix the $(i+1)$ th ambiguity indicates

the float ambiguity \hat{z} is biased away from z , which implies the float baseline $\hat{\mathbf{b}}$ is biased away from \mathbf{b} . If GIAB with $\bar{\mathbf{b}} = \check{\mathbf{b}}_i$ fixes only $i = q < m$ ambiguities, the correction to the float baseline given by (13) is incomplete, leaving some residual bias in $\bar{\mathbf{b}}$. When $\bar{\mathbf{b}}$ is conditioned on the particular value $\check{\epsilon}_{c(i+1)} = \varepsilon \in A_{i+1}$ under Z_i , the bias manifests as an ε -dependent shift of the mean away from \mathbf{b} . When $\bar{\mathbf{b}}$ is conditioned only on Z_i , the bias manifests as a symmetric exodus of probability density away from \mathbf{b} , leaving no mode at \mathbf{b} . Figures of these distributions will be presented in the next subsection.

Note that the above reasoning is not unique to GIAB: the conditional PDF of $\bar{\mathbf{b}}$ will behave similarly for any data-driven partial ambiguity resolution algorithm that corrects the float baseline with the validated fixes.

V. GIAB VARIANTS

The foregoing conditional PDFs and discussion assume $\bar{\mathbf{b}} = \check{\mathbf{b}}_i$ with $i = q$, which, according to (13), implies the float baseline $\hat{\mathbf{b}}$ is only corrected by the q sequentially-constrained ambiguity residuals $\check{\epsilon}_{c(1:q)}$ that pass validation (those satisfying $|\check{\epsilon}_{c_i}| \leq \beta_i/2$). If $q < m$, the next sequentially-constrained ambiguity residual, $\check{\epsilon}_{c(q+1)}$, is ignored, which means that the component of $\hat{\mathbf{b}}$ that might have been corrected by $\check{\epsilon}_{c(q+1)}$ is left unchanged at its float value. This approach, hereafter called float GIAB, is the typical practice in the existing literature on partial ambiguity resolution. However, the existing literature's calculation of integrity risk IR does not appear to recognize that $\bar{\mathbf{b}} = \check{\mathbf{b}}_q$ is biased as described above [17]–[19].

Setting $\bar{\mathbf{b}} = \check{\mathbf{b}}_q$ (thus ignoring $\check{\epsilon}_{c(q+1)}$) is of course not the only way to handle the first ambiguity that fails validation. This paper considers three variants of GIAB, each distinguished by its treatment of the $(q+1)$ th ambiguity. The first is float GIAB, described above. The second, called MAP GIAB by analogy to maximum *a posteriori* (MAP) estimation, applies the most likely fix candidate, which, given GIAB's operation as defined in [11], is equivalent to choosing $\bar{\mathbf{b}} = \check{\mathbf{b}}_{q+1}$ for $q < m$. While not strictly MAP in the sense of integer least squares, the MAP GIAB solution is MAP conditioned on the correctness of the validated fixes. The PDF $f_{\bar{\mathbf{b}}|\check{\epsilon}_{c(i+1)}, Z_i}(\boldsymbol{\xi}|\varepsilon)$ for $\bar{\mathbf{b}} = \check{\mathbf{b}}_{q+1}$ is the same as that of the float variant (for which $\bar{\mathbf{b}} = \check{\mathbf{b}}_q$), except that all $\boldsymbol{\mu}_k(\varepsilon)$ are shifted by the $(i+1)$ th correction in (13), namely $-Q_{\check{\mathbf{b}}_{i+1}} \frac{\check{\epsilon}_{c(i+1)}}{d_{i+1}}$. Recalling that $\epsilon_{c(i+1)} = \check{\epsilon}_{c(i+1)} + \Delta z$, one notes that the additional correction removes the fractional part from $\epsilon_{c(i+1)}$, leaving

$$\boldsymbol{\mu}_k(\varepsilon) = Q_{\check{\mathbf{b}}_{i+1}} \frac{k}{d_{i+1}} \quad (\text{MAP GIAB}) \quad (34)$$

which is zero if $\Delta z = k = 0$. [The argument ε in $\boldsymbol{\mu}_k(\varepsilon)$ is retained for functional consistency with (23).] Thus, for $\bar{\mathbf{b}} = \check{\mathbf{b}}_{q+1}$, the conditional PDF $f_{\bar{\mathbf{b}}|\check{\epsilon}_{c(i+1)}, Z_i}(\boldsymbol{\xi}|\varepsilon)$ is unbiased about \mathbf{b} if the non-validated fix is correct. MAP GIAB monitors the effect of incorrect fixes on IR by calculating each alternate fix's probability and position domain bias. This approach is similar to the concept of position domain integrity (PDI) in the EPIC and GERAFS algorithms.

The third variant of GIAB, called MMSE GIAB by analogy to minimum mean squared error (MMSE) estimation, computes a weighted average of the MAP GIAB baseline solution and the alternative fixed solutions. Because the baseline corrections are applied linearly, MMSE GIAB's partially-fixed baseline $\bar{\mathbf{b}}$ can be written

$$\bar{\mathbf{b}} = \check{\mathbf{b}}_i - Q_{\check{\mathbf{b}}\check{z}_{c(i+1)}} \frac{\varepsilon + \sum_{j \in \mathbb{Z}} p_j(\varepsilon) j}{d_{i+1}} \quad (\text{MMSE GIAB}) \quad (35)$$

Just as with MAP GIAB, MMSE GIAB is only MMSE in a conditional sense with the additional approximation that the third most likely and subsequent fixes at $i = q + 1$ are negligible. This baseline solution is analogous to the Sequential Best Integer Equivariant (BIE) estimator of [20] and related estimators [21], [22], with the difference that MMSE GIAB limits the number of fixes considered by sizing the aperture according to [11].

The ideal corrected baseline, which has a zero-mean-error PDF if $\Delta z = k$, is

$$\bar{\mathbf{b}}_{\text{ideal}} = \check{\mathbf{b}}_i - Q_{\check{\mathbf{b}}\check{z}_{c(i+1)}} \frac{\varepsilon + k}{d_{i+1}} \quad (36)$$

The bias in the MMSE solution is thus

$$\begin{aligned} \boldsymbol{\mu}_k(\varepsilon) &= \bar{\mathbf{b}} - \bar{\mathbf{b}}_{\text{ideal}} \quad (\text{MMSE GIAB}) \\ &= Q_{\check{\mathbf{b}}\check{z}_{c(i+1)}} \frac{k - \sum_{j \in \mathbb{Z}} j p_j(\varepsilon)}{d_{i+1}} \\ &= Q_{\check{\mathbf{b}}\check{z}_{c(i+1)}} \frac{\sum_{j \in \mathbb{Z}} (k - j) p_j(\varepsilon)}{d_{i+1}} \end{aligned} \quad (37)$$

where the last equality makes use of $\sum_{j \in \mathbb{Z}} p_j(\varepsilon) = 1$.

For small values of ε , $p_0(\varepsilon) \gg p_j(\varepsilon)$, $\forall j \neq 0$, meaning that the MAP fix is much more likely than the alternatives, in which case the MMSE and MAP GIAB baselines will differ only slightly. At the other extreme, in the zero-probability event that $|\check{z}_{c(i+1)}| = 1/2$, the MMSE and float GIAB baselines are equivalent.

Analysis has shown that when $P_{C_{i+1}} > 0.7$, which is attainable for even relatively weak models, neglecting all but the two most likely fix candidates for the $(i + 1)$ th ambiguity raises the integrity risk by less than $P_{E_{i+1}}$ for all values of d_{i+1} . This makes the third most likely fix, and all less likely fixes, negligibly likely. In particular, when $P_{C_{i+1}} > 0.7$ the three highest values of $p_k(\varepsilon)$ are $p_0(\varepsilon) > p_{-\text{sgn}(\varepsilon)}(\varepsilon) \gg p_{\text{sgn}(\varepsilon)}(\varepsilon)$. Neglecting all but the two most likely fixes, the partially-fixed baseline $\bar{\mathbf{b}}$ for each of the three GIAB variants can be approximated by the following conditional PDF, with $\boldsymbol{\mu}_k(\varepsilon)$ given by (23), (34), or (37), as appropriate:

$$f_{\bar{\mathbf{b}}|\check{z}_{c(i+1)}, Z_i}(\boldsymbol{\xi}|\varepsilon) \approx \sum_{k \in \{0, -\text{sgn}(\varepsilon)\}} p_k(\varepsilon) \cdot \mathcal{N}(\boldsymbol{\xi}; \bar{\mathbf{b}} + \boldsymbol{\mu}_k(\varepsilon), Q_{\bar{\mathbf{b}}\bar{\mathbf{b}}}) \quad (38)$$

The PDFs of (38), (18), and (15) are illustrated in Figs. 2, 3, and 4, respectively. The PDFs have been shifted so the horizontal axis's origin coincides with the component value of the true baseline \mathbf{b} . Note that the MMSE GIAB PDF in Fig. 2 lies between those of the MAP and float variants. Note also that the float GIAB PDF in Fig. 3 is bimodal, with both modes shifted away from zero, whereas both MAP and MMSE GIAB

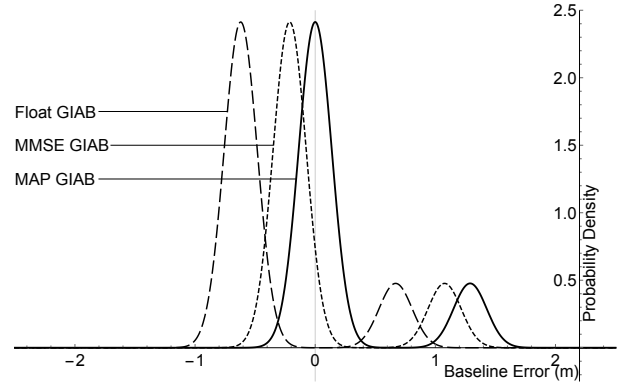


Fig. 2: A single component of $f_{\bar{\mathbf{b}}|\check{z}_{c(i+1)}, Z_i}(\mathbf{b} + \boldsymbol{\xi}|\varepsilon)$ from (38) for float, MAP, and MMSE GIAB for $q = i < m$ and a large ambiguity residual ε . Because the distributions differ only by the variant-specific bias $\boldsymbol{\mu}_k(\varepsilon)$, the three PDFs are merely shifted versions of each other, with that of MMSE GIAB between those of float and MAP GIAB.

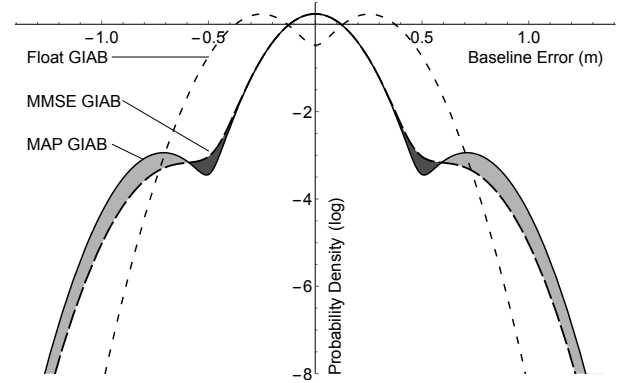


Fig. 3: A single component of $f_{\bar{\mathbf{b}}|Z_i}(\mathbf{b} + \boldsymbol{\xi})$ for float, MAP, and MMSE GIAB with $q = i < m$, plotted with a log-scaled vertical axis. Float GIAB has a symmetric, bimodal PDF. MAP GIAB has a symmetric PDF with a dominant, zero-mean central mode and heavy tails due to incorrect fixes. MMSE GIAB has a lower probability of large errors than does MAP GIAB at the expense of a slight increase in the probability of moderately-sized errors. In the lightly-shaded region, MAP GIAB has higher density than MAP GIAB, and vice versa in the darker region.

have strong modes at zero but wider tails. Finally, observe from Figs. 3 and 4 that MMSE GIAB has narrower tails than MAP GIAB. This is because MAP GIAB does not change its baseline estimate for large residuals like MMSE GIAB does.

VI. VALIDATION OF BASELINE DISTRIBUTIONS

In recognition of the possibility that the previously-derived conditional PDFs of $\bar{\mathbf{b}}$ suffer from some error in reasoning or probabilistic book-keeping, extensive Monte Carlo simulations were conducted to cross-check the analytical expressions. A float solution model was chosen with eight satellites above a 5° mask. The simulation was initialized by computing the decorrelating Z-transform and setting the integer aperture

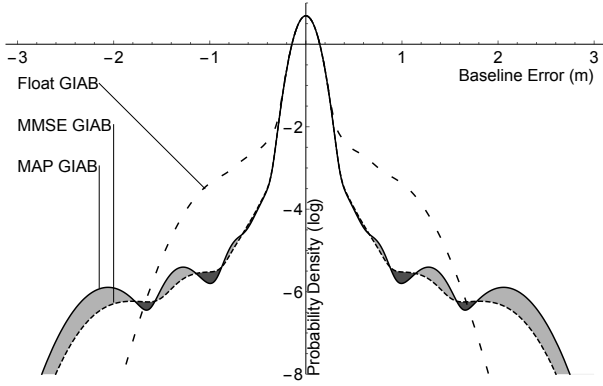


Fig. 4: A single component of $f_{\bar{b}|F^c}(\mathbf{b} + \boldsymbol{\xi})$ for float, MAP, and MMSE GIAB, plotted with a log-scaled vertical axis. Float GIAB has strong but narrow tails. Its central mode results from the probability of fixing all m ambiguities. MAP and MMSE GIAB both have a strong central mode and tails that are wider but lower than those of float GIAB. MMSE GIAB has smoother and narrower tails than MAP GIAB.

according to the optimization described in [11]. A total of 4×10^8 Monte Carlo samples were then drawn from the float distribution described by (2) to generate the float solution errors, including the float baseline and float ambiguities. To save computation time, rather than using sampling in the measurement domain and computing float solutions, the float solution was sampled directly since the float solution is well validated. Multiple models of varying strength were evaluated, but only a single model is presented here to save space. Each sample float ambiguity vector was then Z-transformed and fed through the GIAB algorithm. All GIAB outputs were logged, including the number of correctly fixed samples, the number of incorrectly fixed samples, and the partially-fixed baseline error tabulated by q .

Appropriate histograms of the simulated outcomes were then compared with the analytical PDFs for $f_{\bar{b}|F^c}(\boldsymbol{\xi})$, $f_{\bar{b}|Z_i}(\boldsymbol{\xi})$, and $f_{\bar{b}|\xi_c(i+1), Z_i}(\boldsymbol{\xi}|\varepsilon)$ and for float, MAP, and MMSE GIAB. Fig. 5 shows excellent agreement between the empirical (simulated) and analytical $f_{\bar{b}|F^c}(\boldsymbol{\xi})$ for MAP GIAB. Similarly good agreement was found with the other two distributions and the other two GIAB variants. The model underlying Fig. 5 is relatively strong: its integer bootstrapping probability of correct fix is $1 - 2 \times 10^{-5}$ for a specified failure probability $\bar{P}_F = 10^{-8}$. Several weak models and other strong models were also studied, all of varying geometry. Each case showed excellent agreement with the derived PDFs.

VII. DATA-DRIVEN POSITION DOMAIN INTEGRITY

The defining characteristic of high-integrity CDGNSS techniques appropriate for safety-of-life systems is their ability to strictly bound the probability of large position domain errors (errors in the estimate of the baseline vector \mathbf{b}) even in the event of incorrect fixes. This is the essence of position domain integrity (PDI). For each component of \mathbf{b} , the risk R that the component's error exceeds the AL must be monitored. Let

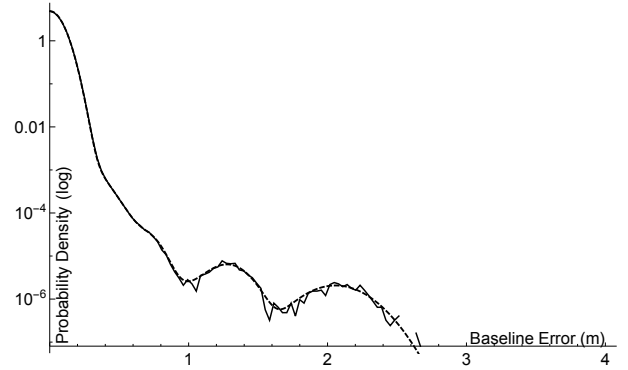


Fig. 5: A single component of $f_{\bar{b}|F^c}(\mathbf{b} + \boldsymbol{\xi})$ for the theoretical PDF of MAP GIAB (dashed line) and the empirical (simulated) histogram (solid line), plotted in log scale for $m = 7$, $\bar{P}_F = 10^{-8}$, and a Monte Carlo sample size of 4×10^8 . The underlying model has an IB probability of correct fix equal to $1 - 2 \times 10^{-5}$. As the PDFs are symmetric about zero, only the positive portion is shown. Clearly, there is strong agreement between the analytical and simulated distributions. Note that because the plot's vertical axis is log scaled, small differences are exaggerated at low probabilities.

b represent a particular component of \mathbf{b} and \bar{b} its estimate, whether fully or partially fixed. Then R is defined as

$$R \triangleq P(|\bar{b} - b| > AL) \quad (39)$$

If $R > \bar{I}R$, where $\bar{I}R$ is a specified integrity risk, an alert must be raised.

A. Position Domain Integrity in EPIC

The EPIC algorithm protects solution integrity by evaluating the *a priori* conditional IR for the case that the ambiguities are fixed correctly and for s cases of incorrect fix. This subsection is a brief, but needed, summary of relevant prior work. [2], [4]. EPIC produces tighter bounds on IR than GERAFS for any error model, so EPIC is considered to the exclusion of GERAFS in this paper. Define \mathcal{E}_0 as the event that the chosen ambiguity fix is correct, and \mathcal{E}_k as the event that the k th alternative fix is correct. Let $R_k = P(|\bar{b} - b| > AL | \mathcal{E}_k) \leq 1$ be the conditional risk of excess error given the event \mathcal{E}_k . The total risk is then

$$R = \sum_{k=0}^s R_k P(\mathcal{E}_k) + \sum_{k=s+1}^{\infty} R_k P(\mathcal{E}_k) \quad (40)$$

Define \mathcal{E}_{∞} as the event that the correct fix was neither the chosen fix nor among the s alternative fix candidates; i.e.,

$$\mathcal{E}_{\infty} \triangleq \bigcup_{k=s+1}^{\infty} \mathcal{E}_k = \left(\bigcup_{k=0}^s \mathcal{E}_k \right)^c \quad (41)$$

where $(\cdot)^c$ indicates the set complement.

A bound on the risk of excess error can be derived by conservatively assuming that any incorrect fix not among the s considered will cause excess error, i.e., assuming $R_k =$

1, $\forall k > s$. This leads to the bound used by EPIC to monitor risk of excess error:

$$\begin{aligned} R_{\text{EPIC}} &\leq P(\mathcal{E}_\infty) + \sum_{k=0}^s R_k P(\mathcal{E}_k) \\ &\leq 1 - \sum_{k=0}^s P(\mathcal{E}_k) + \sum_{k=0}^s R_k P(\mathcal{E}_k) \quad (42) \\ &\leq 1 - \sum_{k=0}^s (1 - R_k) P(\mathcal{E}_k) \end{aligned}$$

In the EPIC algorithm, the event probabilities are the *a priori* fixing probabilities for IB:

$$P(\mathcal{E}_k) = \prod_{j=1}^m \left(\Phi \left(\frac{\frac{1}{2} - L_j^{-1} \Delta \mathbf{z}_k}{\sqrt{d_j}} \right) - \Phi \left(\frac{-\frac{1}{2} - L_j^{-1} \Delta \mathbf{z}_k}{\sqrt{d_j}} \right) \right) \quad (43)$$

where $\Delta \mathbf{z}_k$ is the k th candidate fix ambiguity error vector and L_j^{-1} is the j th row of the matrix L^{-1} . Assuming zero-mean Gaussian measurements, the conditional PDI risk for excess error in a particular direction is

$$R_k = \Phi \left(\frac{AL - \mu_k}{\sigma_{\bar{b}}} \right) - \Phi \left(\frac{-AL - \mu_k}{\sigma_{\bar{b}}} \right) \quad (44)$$

where μ_k is the desired component of the bias in (11) for fix error vector $\Delta \mathbf{z}_k$, and $\sigma_{\bar{b}}^2$ is the variance of that component.

B. Position Domain Integrity in GIAB

Position domain integrity in the GIAB framework enjoys a key advantage over that for EPIC, namely, that GIAB's event probabilities and baseline distributions are *a posteriori* rather than *a priori*. Conditioning on the observed measurements allows GIAB to satisfy the same $\bar{I}R$ as EPIC but with tighter margins. This subsection develops a PDI strategy for GIAB based on the posterior baseline distributions derived previously.

It is important to understand the subtle distinctions in the probabilities of incorrect fix under various conditions. If GIAB's results were only deemed critical in an average sense, then protection based on the *a priori* probability of failure would be sufficient. This is the probability $P_F = P(F) = P(\check{\mathbf{z}}_{1:q} \neq \mathbf{z}_{1:q}, q > 0)$ of validating any incorrect ambiguity. GIAB manages P_F by design, since its aperture vector β is chosen to satisfy $P_F \leq \bar{P}_F$,

But safety-of-life systems are concerned not only with average behavior but also with each estimation epoch's potential for dangerously large errors. Employing a measurement-conditioned distribution allows a clearer assessment of the risk at each epoch. Thus, one might wish to make the posterior distribution in (38) the basis for PDI monitoring. But this distribution is conditioned on the event Z_i , requiring $P(Z_i|q=i) = 1 - P(F|q=i)$ be known for operational use. Consider $P(F|q=i)$, which can be written

$$P(F|q=i) = \frac{P(F, q=i)}{P(F^c, q=i) + P(F, q=i)}, \quad i > 0 \quad (45)$$

The first term in the denominator may be recognized as the probability of correctly validating the first i ambiguities, or

P_{S_i} . The other term, $P(F, q=i)$, is the probability that one or more of i validated ambiguities are incorrect. Since the event $(F, q=i)$ is a subset of the failure event F , it must have a lower probability; thus $P(F, q=i) = \alpha P_F$, where $0 < \alpha < 1$ for $i > 0$. Then

$$P(F|q=i) = \frac{\alpha P_F}{P_{S_i} + \alpha P_F} \approx \frac{\alpha P_F}{P_{S_i}}, \quad i > 0 \quad (46)$$

where the conservative approximation follows from $P_{S_i} \gg P_F$, which is typical for high-integrity systems. For $q=m$ and a strong model, P_{S_m} is very close to unity, so $P(F|q=m)$ remains close to P_F . However, for $q=i < m$ and a strong model, P_{S_i} might itself be quite small, say, less than 10^{-3} , making $P(F|q=i)$ orders of magnitude larger than P_F . In other words, for a strong model, conditioning only on $q < m$ makes an incorrect fix in the q validated ambiguities appear too likely. This would almost certainly cause $IR > \bar{I}R$, triggering an alert and rendering the solution useless.

A more precise assessment of position integrity in such a situation requires a different approach, one based on examination of the full *a posteriori* probabilities of both the correct fix and a large number of potential incorrect fixes. Denote the posterior fixing probability as

$$P(\mathcal{E}_\zeta | \varepsilon, i) \triangleq P(\Delta \mathbf{z} = \zeta | \check{\varepsilon}_c = \varepsilon, q=i) \quad (47)$$

Note that, unlike (31), this expression is not conditioned on Z_i ; i.e., it does not assume that validated fixes are correct. As argued earlier, under Z_i , only two alternative fixes need be considered to approximate the conditional baseline distribution as (31). But in operation, one does not know whether Z_i holds, and so must consider two alternatives *for each ambiguity*, assuming at each stage that the preceding ambiguities were fixed correctly. Since GIAB's output $\check{\mathbf{z}}$ contains r ambiguities, at least $2^r - 1$ alternatives must be evaluated, or their probabilities, as determined by (47), bounded rigorously.

It is straightforward to derive an expression for $P(\mathcal{E}_\zeta | \varepsilon, i)$. Let $\{\zeta_k\}$ be an ordered, indexed set of all members of \mathbb{Z}^r , with $\zeta_0 \triangleq \mathbf{0}$. Then by the definition of conditional probability,

$$\begin{aligned} P(\mathcal{E}_{\zeta_k} | \varepsilon, i) & \quad (48) \\ &= \lim_{d\varepsilon \rightarrow 0} \frac{P(\varepsilon - d\varepsilon < \check{\varepsilon}_c \leq \varepsilon, \Delta \mathbf{z} = \zeta_k | q=i)}{\sum_{\zeta \in \mathbb{Z}^r} P(\varepsilon - d\varepsilon < \check{\varepsilon}_c \leq \varepsilon, \Delta \mathbf{z} = \zeta | q=i)} \end{aligned}$$

Noting that the measured random variable $\check{\varepsilon}_c \in \mathbb{R}^r$ and the fixing error $\Delta \mathbf{z} \in \mathbb{Z}^r$ are related to the zero-mean Gaussian random variable $\varepsilon_{c(1:r)} \triangleq L_{1:r,1:r}^{-1} \varepsilon_{1:r} \sim \mathcal{N}(\mathbf{0}, D_{1:r,1:r})$ as

$$\begin{aligned} \varepsilon_{c(1:r)} &\triangleq L_{1:r,1:r}^{-1} \varepsilon_{1:r} = L_{1:r,1:r}^{-1} (\hat{\mathbf{z}}_{1:r} - \mathbf{z}_{1:r}) \\ &= L_{1:r,1:r}^{-1} (\hat{\mathbf{z}}_{1:r} - (\check{\mathbf{z}} - \Delta \mathbf{z})) \\ &= L_{1:r,1:r}^{-1} (\check{\varepsilon} + \Delta \mathbf{z}) \\ &= \check{\varepsilon}_c + L_{1:r,1:r}^{-1} \Delta \mathbf{z} \end{aligned} \quad (49)$$

and noting that the additional conditioning on the event $q=i$ in (48) restricts the support of $\check{\varepsilon}_c$, but that this only affects the

normalization of the PDF, not its form, then by recognizing equivalent events, (48) can be rewritten as

$$P(\mathcal{E}_{\zeta_k} | \varepsilon, i) = \frac{\mathcal{N}(\varepsilon + L_{1:r,1:r}^{-1} \zeta_k; \mathbf{0}, D_{1:r,1:r})}{\sum_{\zeta \in \mathbb{Z}^r} \mathcal{N}(\varepsilon + L_{1:r,1:r}^{-1} \zeta; \mathbf{0}, D_{1:r,1:r})} \quad (50)$$

$$= \frac{\exp\left(-\frac{1}{2} \|\varepsilon + L_{1:r,1:r}^{-1} \zeta_k\|_{D_{1:r,1:r}}^2\right)}{\sum_{\zeta \in \mathbb{Z}^r} \exp\left(-\frac{1}{2} \|\varepsilon + L_{1:r,1:r}^{-1} \zeta\|_{D_{1:r,1:r}}^2\right)}$$

where $\|\mathbf{x}\|_Q^2 \triangleq \mathbf{x}^T Q^{-1} \mathbf{x}$. Note that (50) can be regarded as generalization of (31) to include additional alternative fix candidates.

The final conditional PDF for $\bar{\mathbf{b}}$ under MAP GIAB, but without conditioning on the correctness of the validated fixes, is a generalization of (38) that includes alternative fixes for more than just the rejected ambiguity, and for each fix, its corresponding position domain bias:

$$f_{\bar{\mathbf{b}}|\bar{\varepsilon}_c, q}(\boldsymbol{\xi} | \varepsilon, i) = \sum_{\zeta_k \in \mathbb{Z}^r} P(\mathcal{E}_{\zeta_k} | \varepsilon, i) \mathcal{N}(\boldsymbol{\xi}; \mathbf{b} + \boldsymbol{\mu}_k, Q_{\bar{\mathbf{b}}_{i+1}}) \quad (51)$$

Each term in the summation corresponds to the event that one of the infinite possible alternative fixes is correct, and accounts for the conditional PDI risk given that event. Each event's baseline remains normally distributed, but with additional mean error caused by the integer offset, as in (11):

$$\boldsymbol{\mu}_k = Q_{\bar{\mathbf{b}}_{\hat{z}_c}} D_{1:r,1:r}^{-1} L_{1:r,1:r}^{-1} \zeta_k \quad (52)$$

A similar expression for $f_{\bar{\mathbf{b}}|\bar{\varepsilon}_c, q}(\boldsymbol{\xi} | \varepsilon, i)$ can be obtained for float and MMSE GIAB. See Appendix D of [23] for details on how to determine which incorrect fixes must be accounted for in (51) and when to truncate the infinite summation in the denominator of (50). The maximum required set of size 2^r , including the IB solution, is obtained by considering the nearest two integers for each ambiguity in a branching tree of alternative solutions. In practice, far fewer than 2^r alternatives need be considered. This represents a significant reduction in computational effort when compared to EPIC.

Let $s \leq 2^r - 1$ be the number of non-negligible alternative fixes considered and the index 0 represent the chosen fix. The IR can be bounded by the following expression, with R_k defined by (44) and with means defined by (52) for MAP GIAB:

$$R_{\text{GIAB}} = 1 - \sum_{k=0}^s (1 - R_k) P(\mathcal{E}_{\zeta_k} | \varepsilon, i) \quad (53)$$

VIII. PERFORMANCE ANALYSIS

A. Protection Levels

Integrity requirements are specified in terms of an integrity risk, \bar{IR} , that the baseline estimation error will exceed the AL threshold without warning. \bar{IR} is derived from an overall risk requirement, such as probability of loss of aircraft, and is typically a fixed value for a given system use case. The AL is related to physical obstacle clearance requirements, which are constant for a particular land based runway and a given aircraft. However, obstacle clearance margins are not constant when landing on a moving platform, such as an

aircraft carrier at sea. Because the risk of excess error is frequently evaluated against a time-varying AL , it is useful to determine a protection level PL that bounds the estimation error to the required level of risk.

PL can be thought of as the minimum AL that could be met by a navigation system or algorithm for a given value of \bar{IR} . In terms of statistical hypothesis testing, \bar{IR} corresponds to the desired confidence level, AL corresponds to the decision threshold, and PL to a prediction interval. If the risk of excess error is expressed as a function of AL , then PL can be defined as

$$PL \triangleq \min_{AL} \{AL | R(AL) \leq \bar{IR}\} \quad (54)$$

PL for EPIC or for any version of GIAB can be computed by using a root solving method to solve (54) with $R(AL)$ defined by (42) or (53), as appropriate.

B. Comparison to EPIC

To demonstrate the performance of GIAB compared to the state-of-the-art high-integrity algorithm, the performance of EPIC and MAP GIAB will be compared for the measurement models previously examined. MAP GIAB is chosen because it provides better accuracy than float GIAB and is simpler to analyze than MMSE GIAB. If MMSE GIAB were used, it would compare even more favorably with EPIC because MMSE GIAB always produces smaller PL values than MAP GIAB.

Because it uses an *a priori*, model driven approach to validation, EPIC will always produce the same PL for the same number of integers fixed with a given measurement model and \bar{IR} . Conversely, GIAB is a data-driven algorithm for which PL is a random variable. PL has a finite support because it is a finite function of the bounded quantity $|\bar{\varepsilon}_{ci}| \leq \frac{1}{2}$.

PL values produced by EPIC will be compared to the minimum, maximum, and average PL produced by GIAB for each number of integers fixed, along with the probability that GIAB will fix that number of integers for each model considered. As shown in Table I with data tabulated from the same Monte Carlo simulations used to generate Fig. 5, GIAB is able to provide smaller PL values than EPIC most of the time. Note that PL computed for U by EPIC is simply the PL of the float solution with no incorrect fixing bias. The event U for GIAB corresponds to the case where the measurements are so poor that no integers can be fixed successfully. The worst case PL computed for any $q > 0$ by MAP GIAB, which has the largest PL s of any of the GIAB implementations, is better than the best PL computed by EPIC.

GIAB provides lower PL s because it is able to reject and exclude most of the incorrect fixes that EPIC must protect against. This implies that GIAB will also provide superior availability of integrity for models similar to those examined in this paper. It is expected that this will be the case in general because the *a posteriori* alternate candidate fix used in GIAB will virtually always be among the candidates considered *a priori* by EPIC. This implies that any decrease in PL computed by EPIC as compared to GIAB will result only when the incorrect fixing bias of the GIAB alternative fix is the same

as the largest incorrect fixing bias considered by EPIC, which will be a rare event.

TABLE I: Integrity performance comparison between EPIC and MAP GIAB. All distance units are in meters. The left-most column indicates the result from GIAB. The next column indicates it's theoretical probability of occurrence [11]. The third column is the standard deviation of the \bar{b} under the given GIAB event. For EPIC, the standard deviations from the previous row applies since GIAB conditions on the first non-validated fix, but EPIC conditions only on the validated fixes. The next three columns indicate the minimum, average and maximum PL produced by GIAB under each event. The final column is the value of PL produced by EPIC when it fixes the same number of integers as GIAB.

\mathcal{E}	$P_{\mathcal{E}}$	σ (m)	PL_{\min}	$\mathbb{E}[PL]$	PL_{\max}	PL_{EPIC}
U	0.00072	0.310	2.79	2.92	3.35	1.77
S_1	0.00043	0.221	1.31	1.32	1.37	2.62
S_2	0.00051	0.196	1.63	1.74	2.13	2.61
S_3	0.00119	0.138	1.75	1.83	2.09	2.49
S_4	0.00090	0.115	1.09	1.16	1.38	3.03
S_5	0.00189	0.084	0.99	1.04	1.20	2.91
S_6	0.00039	0.081	0.48	0.53	0.69	2.99
S_7	0.99393	0.081	0.46	0.46	0.46	2.95

Note that PL values computed by GIAB and EPIC do not increase or decrease uniformly with the number of validated fixes. For example, the maximum PL increases from 1.37 m to 2.13 m when transitioning from the first successful fix to the second successful fix. Recall that PL is driven primarily by the bias between the most likely fix and the incorrect fixes of non-negligible probability. Because these biases depend on the relationships among the various integers and the baseline directions of interest (e.g. vertical error), the biases can change dramatically from one integer fix to the next. Specifically, for EPIC, the case labeled U corresponds to the float solution that includes no incorrect fix biases under the model-driven paradigm.

For both GIAB and EPIC, it is tempting to think that in the case of successfully fixing only two integers in the example above would be better to only fix one integer because that would yield a lower protection level. It may in fact be preferable to do so, but only if the bias induced in the solution by leaving the second integer floating produces acceptable accuracy performance. That is, the reduction in PL is obtained only at the expense of a biased solution that degrades average accuracy. The impact to average accuracy can be seen in the difference between the strength of the central modes of Float and MAP GIAB in Fig. 3.

IX. CONCLUSIONS

A new data-driven CDGNSS partial ambiguity resolution (PAR) and validation algorithm has been developed analytically and validated with Monte Carlo simulation. The new algorithm has advantages over the state-of-the-art in that (1) data-driven methods offer improved availability of integrity over model-driven methods such as EPIC, (2) the integrity risk due to incorrect fixing is bounded analytically as compared to functional approximation methods used with the ratio test and

similar integer aperture methods, (3) it correctly accounts for the integrity risk of PAR in the position domain that existing GIA methods neglect, and (4) it requires less computational burden than EPIC because it eliminates the search for many alternate fix candidates. The new algorithm has been shown to provide superior performance to the current state-of-the-art method for a range of measurement models.

ACKNOWLEDGMENTS

The authors gratefully acknowledge the Naval Air Systems Command (NAVAIR) of the U.S. Navy for supporting this research. However, the opinions discussed here are those of the authors and do not necessarily represent those of the U.S. Navy or any other affiliated agencies. Mr. Green is thankful for the support of his colleagues at Coherent Technical Services, Inc., particularly Surjan Dogra for his insightful reviews of this work. Todd Humphreys's work has been supported by the National Science Foundation under Grant No. 1454474 and by the Data-supported Transportation Operations and Planning Center (DSTOP), a Tier 1 USDOT University Transportation Center.

REFERENCES

- [1] S. Wu, S. R. Peck, R. M. Fries, and G. A. McGraw, "Geometry extraredundant almost fixed solutions: A high integrity approach for carrier phase ambiguity resolution for high accuracy relative navigation," in *ionplans*, 2008, pp. 568–582.
- [2] S. Khanafseh and B. Pervan, "A new approach for calculating position domain integrity risk for cycle resolution in carrier phase navigation systems," in *Proceedings of the IEEE/ION PLANS Meeting*, May 2008, pp. 583–591.
- [3] —, "New approach for calculating position domain integrity risk for cycle resolution in carrier phase navigation systems," *IEEE Transactions on Aerospace and Electronic Systems*, vol. 46, no. 1, pp. 296–307, 2010.
- [4] S. Khanafseh, M. Joerger, and B. Pervan, "Integrity risk of cycle resolution in the presence of bounded faults," in *Proceedings of the IEEE/ION PLANS Meeting*, April 2012, pp. 664–672.
- [5] S. Khanafseh and B. Pervan, "Detection and mitigation of reference receiver faults in differential carrier phase navigation systems," *IEEE Transactions on Aerospace and Electronic Systems*, vol. 47, no. 4, pp. 2391–2404, Oct. 2011.
- [6] B. Decléene, "Defining pseudorange integrity - overbounding," in *Proceedings of the ION GPS Meeting*, September 2000, pp. 1916–1924.
- [7] P. Teunissen, "Integer aperture GNSS ambiguity resolution," *Artificial Satellites*, vol. 38, no. 3, pp. 79–88, 2003.
- [8] P. J. G. Teunissen, "The probability distribution of the ambiguity bootstrapped gnss baseline," *Journal of Geodesy*, vol. 75, no. 5-6, pp. 267–275, 2001. [Online]. Available: <http://dx.doi.org/10.1007/s001900100172>
- [9] P. Teunissen, P. De Jonge, and C. Tiberius, "The least-squares ambiguity decorrelation adjustment: its performance on short GPS baselines and short observation spans," *Journal of geodesy*, vol. 71, no. 10, pp. 589–602, 1997.
- [10] P. Teunissen, "Integer aperture bootstrapping: a new GNSS ambiguity estimator with controllable fail-rate," *Journal of Geodesy*, vol. 79, no. 6-7, pp. 389–397, 2005. [Online]. Available: <http://dx.doi.org/10.1007/s00190-005-0481-y>
- [11] G. N. Green and T. E. Humphreys, "Data-driven generalized integer aperture bootstrapping for high-integrity positioning," *IEEE Transactions on Aerospace and Electronic Systems*, 2017, submitted for review. [Online]. Available: <http://goo.gl/pfq9EU>
- [12] G. N. Green, M. King, and T. E. Humphreys, "Data-driven generalized integer aperture bootstrapping for real-time high integrity applications," in *Proceedings of the IEEE/ION PLANS Meeting*, Savannah, GA, 2016.
- [13] P. Teunissen, D. Imparato, and C. Tiberius, "Does RAIM with correct exclusion produce unbiased positions?" *Sensors*, vol. 17, pp. 1508–1525, 2017.

- [14] P. J. Teunissen, "The least-squares ambiguity decorrelation adjustment: a method for fast GPS integer ambiguity estimation," *Journal of Geodesy*, vol. 70, no. 1-2, pp. 65–82, 1995.
- [15] M. Psiaki and S. Mohiuddin, "Global positioning system integer ambiguity resolution using factorized least-squares techniques," *Journal of Guidance, Control, and Dynamics*, vol. 30, no. 2, pp. 346–356, March–April 2007.
- [16] P. Teunissen, "Theory of carrier phase ambiguity resolution," *Wuhan University Journal of Natural Sciences*, vol. 8, no. 2, pp. 471–484, 2003. [Online]. Available: <http://dx.doi.org/10.1007/BF02899809>
- [17] A. Brack and C. Gunther, "Generalized integer aperture estimation for partial GNSS ambiguity fixing," *Journal of Geodesy*, vol. 88, no. 5, pp. 479–490, 2014. [Online]. Available: <http://dx.doi.org/10.1007/s00190-014-0699-7>
- [18] A. Brack, "On reliable data-driven partial GNSS ambiguity resolution," *GPS Solutions*, vol. 19, no. 3, pp. 411–422, 2015. [Online]. Available: <http://dx.doi.org/10.1007/s10291-014-0401-9>
- [19] Y. Hou, S. Verhagen, and J. Wu, "A data driven partial ambiguity resolution: Two step success rate criterion, and its simulation demonstration," *Advances in Space Research*, vol. 58, no. 11, pp. 2435 – 2452, 2016. [Online]. Available: <http://www.sciencedirect.com/science/article/pii/S0273117716303994>
- [20] A. Brack, P. Henkel, and C. Günther, "Sequential best integer-equivariant estimation for GNSS," *Navigation*, vol. 61, no. 2, pp. 149–158, 2014.
- [21] P. Teunissen, "Theory of integer equivariant estimation with application to GNSS," *Journal of Geodesy*, vol. 77, pp. 402–410, 2003.
- [22] Z. Wen, P. Henkel, A. Brack, and C. Gnther, "Best integer equivariant estimation for precise point positioning," in *ELMAR, 2012 Proceedings*, Sept 2012, pp. 279–282.
- [23] G. N. Green, "Advanced techniques for safety-of-life carrier phase differential GNSS positioning with applications to triplex architectures," Ph.D. dissertation, The University of Texas at Austin, Dec. 2017. [Online]. Available: <https://goo.gl/zWc2SH>